NASA TECHNICAL NOTE

NASA TN D-6106

c.1

NASA TN D-6106

VIBRATION AND FLUTTER TESTS OF A PRESSURIZED THIN-WALLED TRUNCATED CONICAL SHELL

by Robert Miserentino and Sidney C. Dixon

Langley Research Center
Hampton, Va. 23365

NATIONAL AERONAUTICS AND SPACE ADMINISTRATION • WASHINGTON, D. C. • FEBRUARY 1971

1. Report No.	2. Government Accession No.	3. Recipient's Catalog No.
NASA TN D-6106		

4. Title and Subtitle	5. Report Date
VIBRATION AND FLUTTER TESTS OF A PRESSURIZED THIN-WALLED TRUNCATED CONICAL SHELL	February 1971
	6. Performing Organization Code
7. Author(s)	8. Performing Organization Report No.
Robert Miserentino and Sidney C. Dixon	L-7345
	10. Work Unit No.
9. Performing Organization Name and Address	124-08-20-04
NASA Langley Research Center Hampton, Va. 23365	11. Contract or Grant No.
	13. Type of Report and Period Covered
12. Sponsoring Agency Name and Address	Technical Note
National Aeronautics and Space Administration Washington, D.C. 20546	14. Sponsoring Agency Code

15. Supplementary Notes

16. Abstract

The breathing vibration modes of an unstiffened truncated conical shell have been determined and the shell was tested for flutter at a Mach number of 3.0 in the Langley 9- by 6-foot thermal structures tunnel. The shell was made of stainless steel and had a ratio of length to large radius of 3.72, a ratio of large radius to thickness of 811, and a semivertex angle of 0.26 rad (15°). Experimental results are presented to show the variations of resonant frequency with internal pressure and with circumferential wave number. For sufficiently large pressures and a small number of circumferential waves, the variation of frequency squared with pressure departed from its originally linear characteristic. The experimental results compared favorably with the calculated results although the theory tended to overestimate the frequency increase which resulted from an increase in internal pressure. The theory did not predict the nonlinear variation of frequency squared with pressure. A flutter point obtained in the wind-tunnel test is compared with a flutter boundary calculated from an analysis based on a Donnell-type theory. The relationship between experiment and theory is similar to the trends previously established for cylindrical shells.

17. Key Words (Suggested by Author(s))	18. Distribution Statement
Shell flutter Conical shell Natural vibrations of pressurized cone	Unclassified – Unlimited

19. Security Classif. (of this report)	20. Security Classif. (of this page)	21. No. of Pages	22. Price*
Unclassified	Unclassified	24	$3.00

*For sale by the National Technical Information Service, Springfield, Virginia 22151

VIBRATION AND FLUTTER TESTS OF A PRESSURIZED THIN-WALLED TRUNCATED CONICAL SHELL

By Robert Miserentino and Sidney C. Dixon
Langley Research Center

SUMMARY

The breathing vibration modes of an unstiffened truncated conical shell have been determined and the shell was tested for flutter at a Mach number of 3.0 in the Langley 9- by 6-foot thermal structures tunnel. The shell was made of stainless steel and had a ratio of length to large radius of 3.72, a ratio of large radius to thickness of 811, and a semivertex angle of 0.26 rad (15°).

Experimental results are presented to show the variations of resonant frequency with internal pressure and with circumferential wave number. For sufficiently large pressures and a small number of circumferential waves, the variation of frequency squared with pressure departed from its originally linear characteristic. The experimental results compared favorably with the calculated results although the theory tended to overestimate the frequency increase which resulted from an increase in internal pressure. The theory did not predict the nonlinear variation of frequency squared with pressure.

A flutter point obtained in the wind-tunnel test is compared with a flutter boundary calculated from an analysis based on a Donnell-type theory. The relationship between experiment and theory is similar to the trends previously established for cylindrical shells.

INTRODUCTION

Circular conical shells are presently being used as primary structures for launch vehicles and spacecraft. Consequently, the vibration and flutter characteristics of such shells are of prime importance to the designer.

There has been considerable research on the vibration of conical shells, most of which is summarized in the comprehensive survey of the literature given in reference 1. Most of these previous investigations were theoretical analyses of unpressurized shells and were restricted to specified classical boundary conditions (usually cantilevered or simply supported). The more limited experimental data available are for unpressurized

MODEL, APPARATUS, AND TESTS

Model

The model was a truncated conical shell with a semivertex angle α of 0.26 rad (15°). The model was constructed from 17-7 PH stainless steel, and had a nominal ratio of large radius to thickness of 811 and a ratio of length to large radius of 3.72. Assembly details, physical properties, and dimensions of the model are given in figure 1. To facilitate wind-tunnel testing, a pointed solid nose tip was attached to the small end of the model so that the shell and nose tip comprised a complete cone. The large end of the model was attached to a bulkhead which was a 1.9-cm-thick (0.75-in.) steel disk with a 1.3-cm-thick (0.5-in.) cylindrical flange. The cone material was fitted and welded to two cylindrical doublers. The cylindrical doublers were sealed on the flange with an elastomer bonding material and held in place with 94 screws. The cone was cut from three sheets, rolled, and seam welded in the pattern shown in figure 1.

Test Apparatus

Fixture.- The fixture used to support the cone for the vibration tests consisted of a sting rigidly bolted to the bulkhead and mounted on a gooseneck sting support as shown in figure 2. The only change in the fixture for the wind-tunnel tests was to use a cross-sting support as shown in figure 3.

Shell pressurizing system.- A regulated compressed-air source was used to pressurize the shell for vibration tests. A Bourdon tube pressure gage was used to measure the internal pressure. The gage was accurate to within one-half of 1 percent of the scale value, and zero shifts during a test were less than one division of the gage, 34 N/m^2 (0.005 psi). For the tunnel tests, three solenoid-operated valves were mounted on the inside wall of the bulkhead. Two 2.5-cm-diameter (1-in.) globe valves were used to vent the internal pressure to the pressure level behind the bulkhead, and a 1.9-cm-diameter (3/4-in.) valve, attached to a 680 kN/m^2 (100 psi) source was used for pressurization. A direct reading electrical pressure gage was also mounted on the inside wall of the bulkhead and was monitored during the run, and the output was recorded. The combined accuracy of the gage and reading system was 340 N/m^2 (0.05 psi). The electrical pressure gage was also connected to an automatic pressure control system with a manual override.

Vibration equipment.- An electromagnetic shaker was used to excite harmonic vibrations of the shell. (See fig. 2.) The shaker placement and frequency were varied until the desired mode was obtained. The shell deflections around the circumference were measured with a variable-reluctance pickup at a point 0.44 of the length of the shell from the large end. The variable-reluctance pickup was chosen because it does not contact the model. The pickup was rotated around the shell on a motor-driven ring at the rate of 1 rpm. The pickup was automatically positioned radially to the desired distance from the shell wall by a servosystem. Thus, any variations in circularity or misalinement of the pickup support did not affect the amplitude of the ac signal produced by the vibrating shell. Longitudinal variations in the response deflections were measured at low pressure only with a handheld velocity probe with a spring constant of 3.4 N/m (0.02 lbf/in.). The frequency of the pickup signal was read on a stroboscopic frequency meter.

Wind tunnel.- The wind-tunnel test was conducted in the Langley 9- by 6-foot thermal structures tunnel, a Mach 3 intermittent blowdown facility exhausting to the atmosphere. A heat exchanger was preheated to provide stagnation temperatures from about 310 K to 620 K (100° F to 660° F). The stagnation pressure can be varied from about 410 to 1380 kN/m^2 (60 to 200 psia). Additional details on the tunnel are presented in reference 5.

Flutter test instrumentation.- Fixed to the inside of the shell and ramdomly spaced were 4 single active arm strain gages and 12 thermocouples. In addition, there were 8 deflectometer gages mounted on a stiff frame cantilevered from the bulkhead. They were placed on diametric lines, four per line, and equally spaced about 16.5 cm (6.5 in.) apart. At the time the flutter occurred only 5 deflectometers were working.

Test Procedure

Vibration tests.- Data were obtained by setting the internal pressure and varying the frequency. The ac output of the vibration pickup was displayed on an oscilloscope along with the shaker input signal to obtain a Lissajous ellipse. Resonance was taken to be a peak amplitude response on the oscilloscope. At each resonant frequency, the variable-reluctance pickup was driven around the cone to determine the spacing and number of circumferential waves. The modes are denoted herein by a double index, n for the number of waves around the circumference and m for the number of half-waves in the longitudinal direction.

Wind-tunnel test.- The wind-tunnel tests were conducted at a Mach number of 3, at a dynamic pressure of 67 to 240 kN/m^2 (1400 to 5000 psf), and at a stagnation temperature of 422 K (300° F). The internal pressure in the shell was maintained at 179 kN/m^2 (26 psi) absolute during the first 5 seconds of the tests in order to prevent damage during the tunnel start-up and settling out period. During the remainder of the test, the model internal pressure was generally decreasing with time.

RESULTS AND DISCUSSION

Vibration

Experimental results.- The measured pressures and resonant frequencies for all recorded breathing vibration modes (for $m = 1$) are given in table I and are shown in figure 4 in terms of the nondimensional frequency parameter $(\omega/\omega_r)^2$ and differential

TABLE I.- MEASURED RESONANT FREQUENCIES FOR $m = 1$

Δp		f, Hz, for n of –											
kN/m^2	psi	2	3	4	5	6	7	8	9	10	11	12	13
0	0	99.3	86.0	83.5	88.0	94.0	102	115	130	149	170	196	225
6.89	1	108	103	103	110	119	130	146	163	185	210	235	
13.78	2	118	117	121	128	139	153	172	194	218	246		
20.68	3	126	128	134	142	154	171	191	214	244	275		300
27.57	4	133	137	145	155	168	187	209	236	270	302		
34.47	5	139	142	152	164	181	202	227	255	292	319	376	
41.36	6	144	147	158	172	192	215	243	273	312			
48.26	7	147	152	163	180	201	228	255	290	334			
55.15	8	148	155	168	185	210	241	272	307	353			
62.05	9	148	158	173	192	220	251	287	324	375	435		
68.94	10	148	161	177	198	228	262	302	346	395	464		
75.84	11	148	163	180		237	271	314	362	420	494		
82.72	12	149			208			326		447			

pressure Δp. Data for values of the wave number n of 2 to 5 are shown in figure 4(a), and data for n from 6 to 10 are shown in figure 4(b). The straight lines are faired through the low Δp data points and pass through the experimental frequency at $\Delta p = 0$. As can be seen from figure 4(a) the variation of $(\omega/\omega_r)^2$ with Δp is linear for small values of Δp ($\Delta p < 35$ kN/m^2 (5 psi)), but is nonlinear for large values of Δp ($\Delta p > 35$ kN/m^2 (5 psi)). The degree of nonlinearity is seen to be dependent on the wave number n. For $n = 2$, $(\omega/\omega_r)^2$ reaches a limiting value at $\Delta p \approx 55$ kN/m^2 (8 psi) and is virtually insensitive to further increases in Δp. As n increases, the nonlinear variations become less pronounced and for $n \geqq 6$, the variation is essentially linear over the entire range of Δp considered.

Comparison with theoretical results.- Theoretical and experimental variations of frequency with wave number n are shown in figure 5 for several values of internal pressure. The theoretical results were obtained from the theory of reference 3. Theoretical curves are shown for three classical boundary restraints: two cases of simply supported edges $\left(N_y = w = M_y = 0\right.$, and either $v = 0$ or $\left.N_{y\theta} = 0\right)$ and clamped edges $\left(u = v = w = \frac{\partial w}{\partial x} = 0\right)$. Changing the supported boundary condition from $v = 0$ to $N_{y\theta} = 0$ has a slight effect for $n \leqq 5$ and essentially no effect for $n > 5$. Clamping the edges had a significant effect over the entire range of n considered, although the effect tends to decrease with increasing n.

For $\Delta p = 0$, the experimental results are in good agreement with the theoretical results for supported edges for $n \geqq 3$. (See fig. 5(a).) At $n = 2$, the experimental value is considerably below the theoretical boundary for supported edges which is the usual result for calculations based on Donnell theory. (See, for example, ref. 6.) Thus, for $\Delta p = 0$, the present experimental model appears to be best represented by simply supported edges. However, the theoretical results tend to overpredict the stiffening effects of increasing Δp as indicated in figures 5(b), 5(c), and 5(d).

The minimum experimental and theoretical frequencies (for simply supported edges) occur at $n = 4$ for $\Delta p = 0$ and $n = 3$ for $\Delta p = 14$ kN/m^2 (2 psi). For $\Delta p > 14$ kN/m^2 (2 psi), the minimum experimental frequency occurs at $n = 2$ whereas the theoretical value remains $n = 3$.

Figure 6 shows the theoretical and experimental variations of $(\omega/\omega_r)^2$ with Δp for $n = 2$, 7, and 10. Application of negative values of Δp resulted in buckling of the conical shell into seven circumferential waves at $\Delta p = -5.5$ kN/m^2 (-0.80 psi), as indicated by the square symbol on the Δp-axis in figure 6. Theoretical results for supported edges indicated buckling into seven waves at $\Delta p = -8.00$ kN/m^2 (-1.16 psi). As can be seen from figure 6, the theory indicates linear variations of $(\omega/\omega_r)^2$ with Δp and tends to overpredict the stiffening influence of internal pressure.

The theoretical results presented in figures 5 and 6 were obtained from the approximate theory of reference 3 which is based on Donnell-type shell theory, neglects inplane inertias, and uses a membrane prestress state. To determine the effect of these approximations, calculations were made by using a rigorous numerical analysis which was recently completed at the Langley Research Center. The analysis is based on Sanders shell theory and the corresponding computer program is called SALORS (Structural Analysis of Layered Orthotropic Ring Stiffened Shells of Revolution). Although not fully documented in the literature, it is briefly described in reference 7. Accurate nonlinear prestress quantities were obtained from the stress analysis section of the computer program which was used as input for the vibration calculations. All results obtained were lower than the results obtained from reference 3 and hence were generally in better agreement with experiment. However, the differences in the results from the two theories were slight (less than about 7 percent) except for $n < 3$ where appreciable differences between results from Donnell and Sanders theory are expected. The results from SALORS indicated no significant change in the linear variation of $(\omega/\omega_r)^2$ with Δp. The agreement between the two theories for vibration indicates that the structural approximation in the analysis using the Donnell theory should not significantly affect the accuracy of the flutter calculations.

Flutter

Experimental results.- The free-stream dynamic pressure and the internal pressure histories for the wind-tunnel tests made on the conical shell are shown in figure 7. Neither the first test nor the start-up and first 18 seconds of the second test caused any visible damage to the model. Not until the last 3 seconds of the second test were any positive flutter results obtained. A sample deflectometer record is shown in figure 8. The deflectometer records indicated the first flutter as a distinct change from a random low-amplitude noise signal to a periodic signal of larger amplitude when $\Delta p = 11.6\ \text{kN/m}^2$ (1.68 psi). A plot of the relative deflectometer output during these 3 seconds is shown in figure 9 as a function of the differential pressure. As the differential pressure continued to decrease, the flutter amplitude increased until it was easily visible in the motion-picture films taken during the test, as indicated in figure 9. The flutter was only briefly visible (about 0.66 second) and then appeared to stop. However, the deflectometers continued to show the shell to be fluttering, although the amplitude was decreased. There was a slight rise in the internal pressure, and then a continual reduction until the flutter increased in amplitude sufficiently to again become visible in the motion pictures. After about 0.10 second of this larger amplitude flutter, permanent deformations with $n = 9$ formed and then the shell collapsed. A close examination of the internal pressure record shows an unexpected decrease at the time that the permanent deformations form; this decrease could be an indication of an unseen crack opening, probably at the base circumferential weld. Frames from the motion pictures indicating the final flutter and initial permanent deformations are shown in figure 10.

The spacing of the node lines in each view at the time of the first permanent deflections was such that $n = 9$. The flutter frequency recorded by the deflectometers was essentially constant throughout the flutter range and remained at 580 Hz. The experimentally observed pattern during the largest amplitude flutter period indicated there were about six circumferential waves and more than one longitudinal half-wave. In contrast to the results for cylinders (ref. 8), circumferentially traveling wave flutter was not observed in the motion pictures or deflectometer records.

The relative deflectometer output shown in figure 9 reveals that decreasing the internal pressure first initiated flutter, then nearly stopped the flutter, and later caused a second significant increase in the flutter amplitude. This trend is similar to the flutter trends obtained for pressurized cylinders (for example, refs. 9 and 10) wherein a shell, initially stable at some value of internal pressure and constant free-stream conditions, undergoes an unstable-stable-unstable cycle as the internal pressure is decreased to zero.

Comparison with theoretical results.- The results of the wind-tunnel tests are compared with a theoretical flutter boundary in figure 11, which gives the variation of the cube root of the flutter parameter λ_L with Δp. The theoretical flutter boundary was calculated for simply supported edges with $v = 0$ from the theory of reference 3. Note that for the range of Δp shown in figure 11, the theoretical predictions of the shell natural frequencies were in good agreement with experiment for $n > 4$ (figs. 5(a) and 5(b)), although theory tended to overpredict the stiffening influence of differential pressure. The theoretical results indicated flutter with 12 circumferential waves at a frequency of 366 Hz. The theoretical flutter boundary does not vary greatly with variations in Δp; this trend was noted previously in reference 3. The flutter boundary was obtained from calculations wherein the effects of aerodynamic damping were neglected; inclusion of the damping would raise the theoretical boundary somewhat.

The results of the wind-tunnel tests are indicated by the dashed line in figure 11. The test conditions at flutter start ($M = 3.0$, $q = 230$ kN/m^2 (33.3 psi)) were such that the local flow conditions over the model were taken to be $M_L = 2.5$ and $q_L = 332.2$ kN/m^2 (48.18 psi). These conditions give an experimental flutter point of ${\lambda_L}^{1/3} = 1.63$ which is well below the theoretical flutter boundary for which ${\lambda_L}^{1/3} = 2.53$. Hence, theory appears to be unconservative, which is also the case for flutter of pressurized cylinders. (See refs. 9 and 10.) Definite conclusions cannot be made, however, since only a single test point is available for comparison with theory.

CONCLUDING REMARKS

Vibration and flutter experiments with a pressurized circular conical shell have been made and the results are compared with theory. The cone was a stainless-steel shell 0.0470 cm (0.0185 in.) thick and had a semivertex angle of 0.26 rad (15°). The ratio of large radius to thickness was 811 and the ratio of length to large radius was 3.72.

For small numbers of circumferential waves, the variation of frequency squared with differential pressure became nonlinear as the differential pressure became large. The experimental results compared favorably with calculated results obtained from an analysis based on Donnell type theory except for modes with two circumferential waves. However, the theory tended to overestimate the frequency increase which resulted from an increase in internal pressure and did not predict the nonlinear variation of frequency squared with pressure. Calculations based on Sanders shell theory and a nonlinear prestress state improved the agreement between theory and experiment somewhat, but again did not predict a nonlinear variation of frequency squared with pressure.

The flutter tests were conducted at Mach 3 in the Langley 9- by 6-foot thermal structures tunnel. The experimental results revealed that decreasing the differential pressure could initiate flutter and suggested that further decreases could stop the flutter. This behavior is not peculiar to conical shells since similar trends have been established for flutter of pressurized cylinders. The experimental flutter results suggested that the theory is unconservative; however, definite conclusions could not be made since only the single test point of this investigation was available for comparison with theory.

Langley Research Center,
National Aeronautics and Space Administration,
Hampton, Va., December 22, 1970.

APPENDIX

CONVERSION OF U.S. CUSTOMARY UNITS TO SI UNITS

Factors required for conversion of the units used herein to the International System (SI) are given in the following table:

Physical quantity	U.S. Customary Unit	Conversion factor (*)	SI Unit (**)
Length, radius	in.	0.0254	meters (m)
Pressure	psi	6.894757×10^3	newtons/meter^2 (N/m^2)
	psf	47.88	newtons/meter^2 (N/m^2)
Density	$\frac{\text{lbf-sec}^2}{\text{in}^4}$	10.69×10^6	kilograms/meter^3 (kg/m^3)
Temperature	$^\circ$F	$\frac{5}{9}(F + 459.67)$	kelvin (K)
Force (load, drag) . . .	lbf	4.44822	newtons (N)
Mass	lbm	0.453 592	kilograms (kg)
Angle	deg	0.01745329	radians (rad)

*Multiply value given in U.S. Customary Unit by conversion factor to obtain equivalent value in SI units.

**Prefixes to indicate multiples of units are as follows:

Prefix	Multiple
kilo (k)	10^3
centi (c)	10^{-2}
milli (m)	10^{-3}
giga (G)	10^9

REFERENCES

1. Hu, William C. L.: A Survey of the Literature on the Vibrations of Thin Shells. Tech. Rep. No. 1 (Contract No. NASr-94(06)), Southwest Res. Inst., June 30, 1964.
2. Weingarten, V. I.: The Effect of Internal and External Pressure on the Free Vibrations of Conical Shells. Int. J. Mech. Sci., vol. 8, no. 2, Feb. 1966, pp. 115-124.
3. Dixon, Sidney C.; and Hudson, M. Latrelle: Flutter, Vibration, and Buckling of Truncated Orthotropic Conical Shells With Generalized Elastic Edge Restraint. NASA TN D-5759, 1970.
4. Comm. on Metric Pract.: ASTM Metric Practice Guide. NBS Handbook 102, U.S. Dep. Com., Mar. 10, 1967.
5. Schaefer, William T., Jr.: Characteristics of Major Active Wind Tunnels at the Langley Research Center. NASA TM X-1130, 1965.
6. Seide, Paul: On the Free Vibrations of Simply Supported Truncated Conical Shells. SSD-TDR-64-15, U.S. Air Force, Feb. 27, 1964. (Available from DDC as AD 600 939.)
7. Anderson, M. S.; Fulton, R. E.; Heard, W. L., Jr.; and Walz, J. E.: Stress, Buckling, and Vibration Analysis of Shells of Revolution. NASA Paper presented at Conference on Computer Oriented Analysis of Shell Structures (Palo Alto, Calif.), Aug. 1970.
8. Olson, Mervyn D.; and Fung, Y. C.: Supersonic Flutter of Circular Cylindrical Shells Subjected to Internal Pressure and Axial Compression. AIAA J., vol. 4, no. 5, May 1966, pp. 858-864.
9. Olson, Mervyn D.; and Fung, Y. C.: Comparing Theory and Experiment for the Supersonic Flutter of Circular Cylindrical Shells. AIAA J., vol. 5, no. 10, Oct. 1967, pp. 1849-1856.
10. Barr, Gerald W.; and Stearman, Ronald O.: Aeroelastic Stability Characteristics of Cylindrical Shells Considering Imperfections and Edge Constraint. AIAA J., vol. 7, no. 5, May 1969, pp. 912-919.

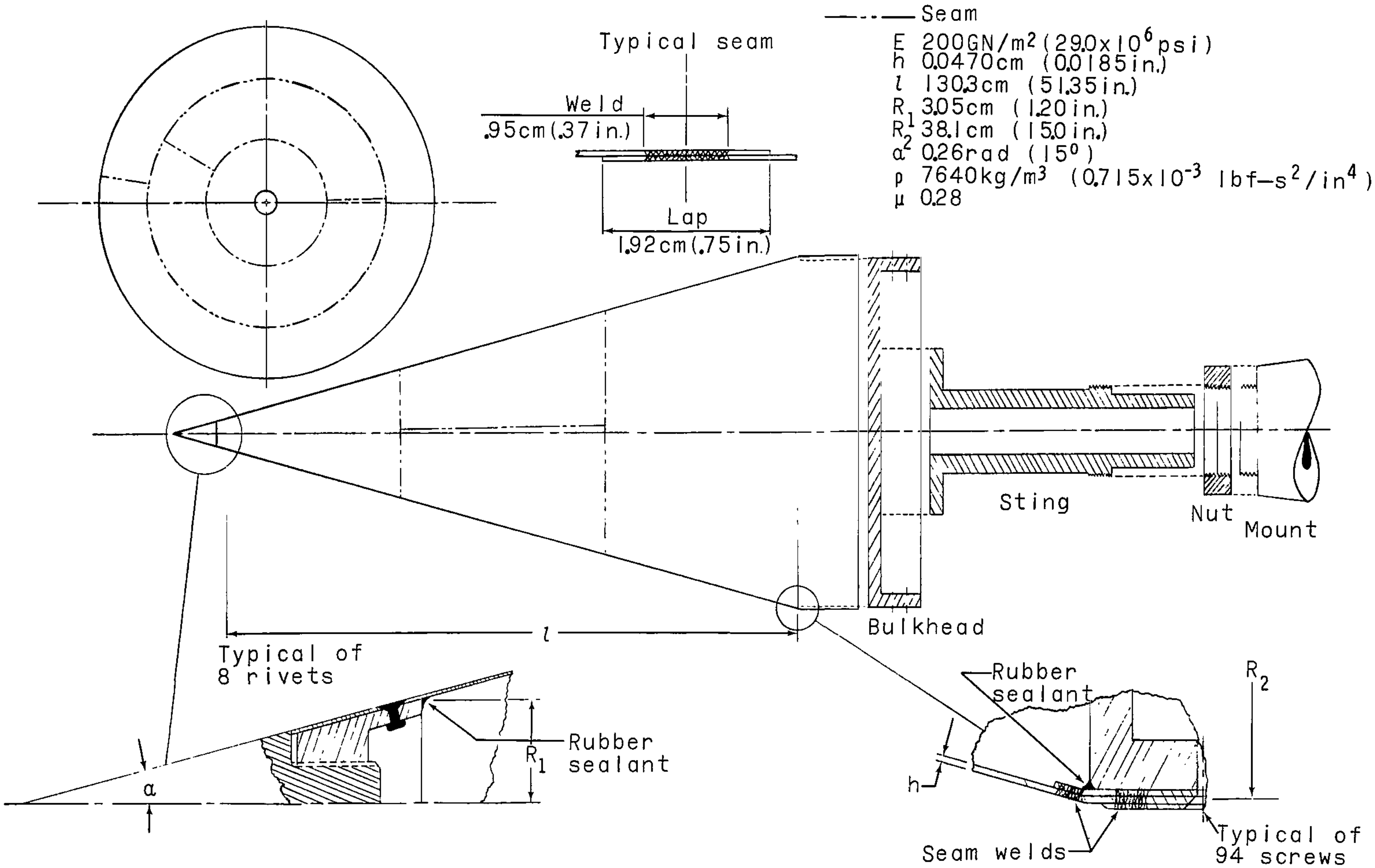

Figure 1.- Physical properties, assembly details, and dimensions of conical shell.

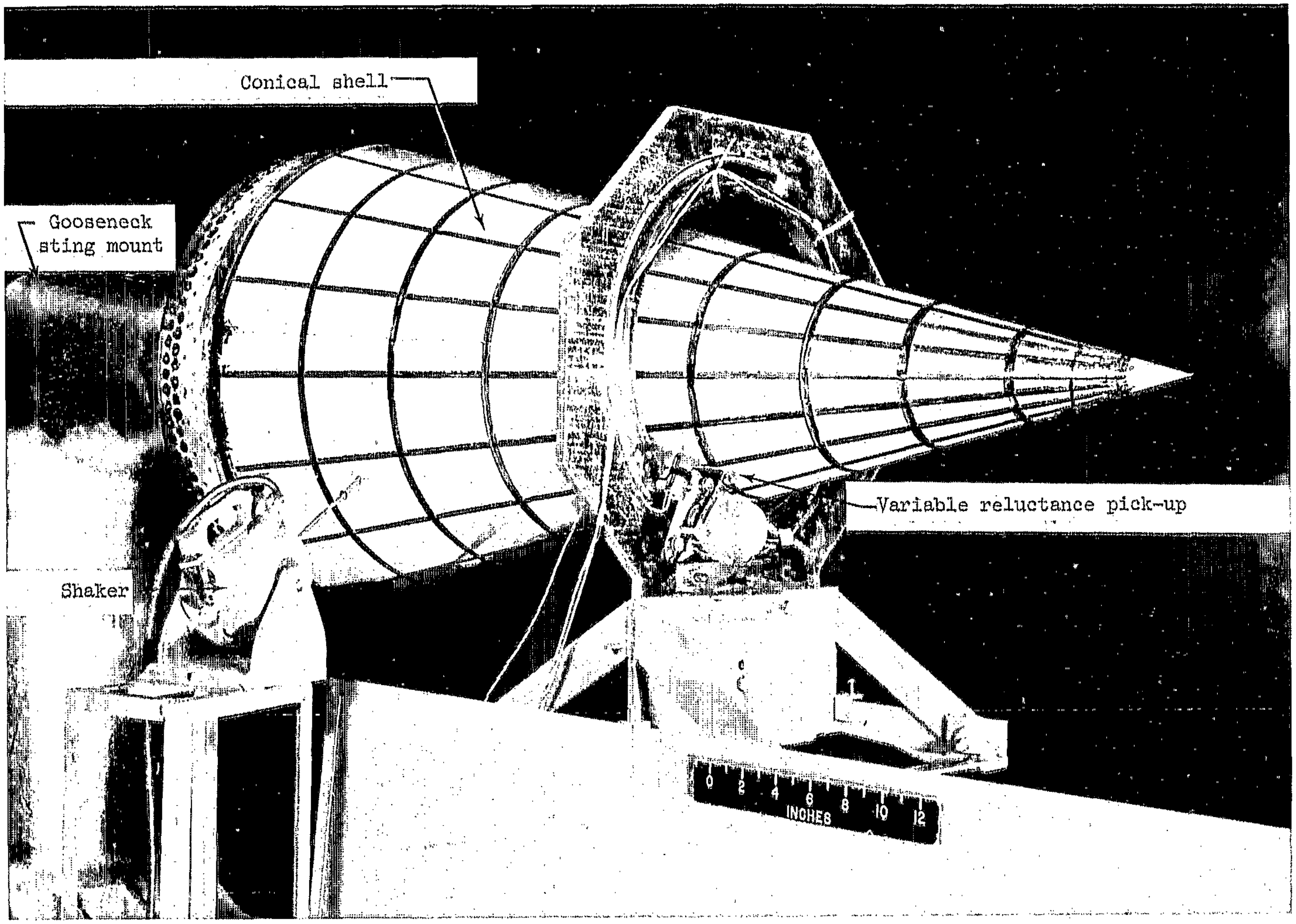

L-60-582.1

Figure 2.- Vibration test setup.

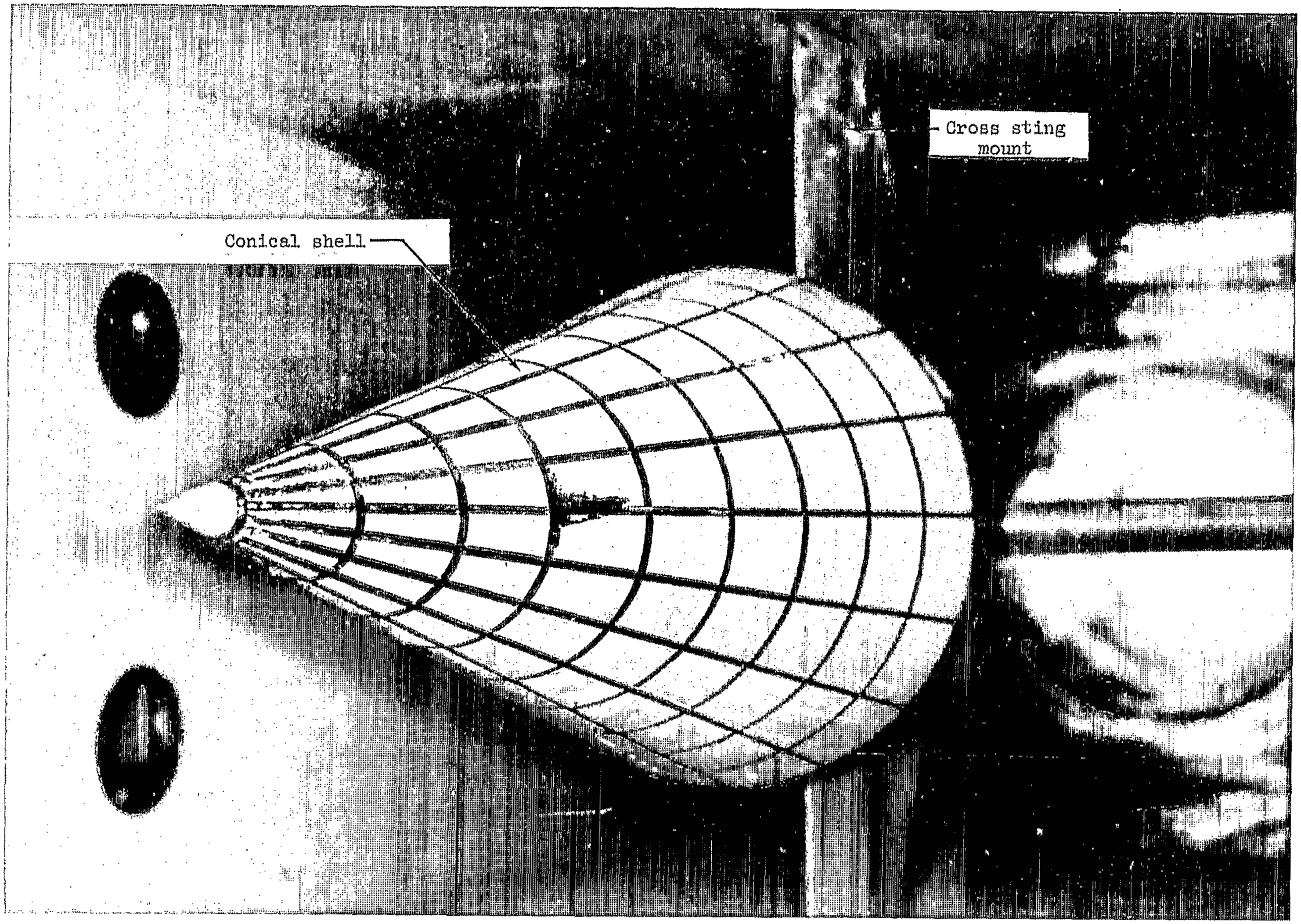

L-61-4384.1

Figure 3.- Conical shell mounted in wind-tunnel test section.

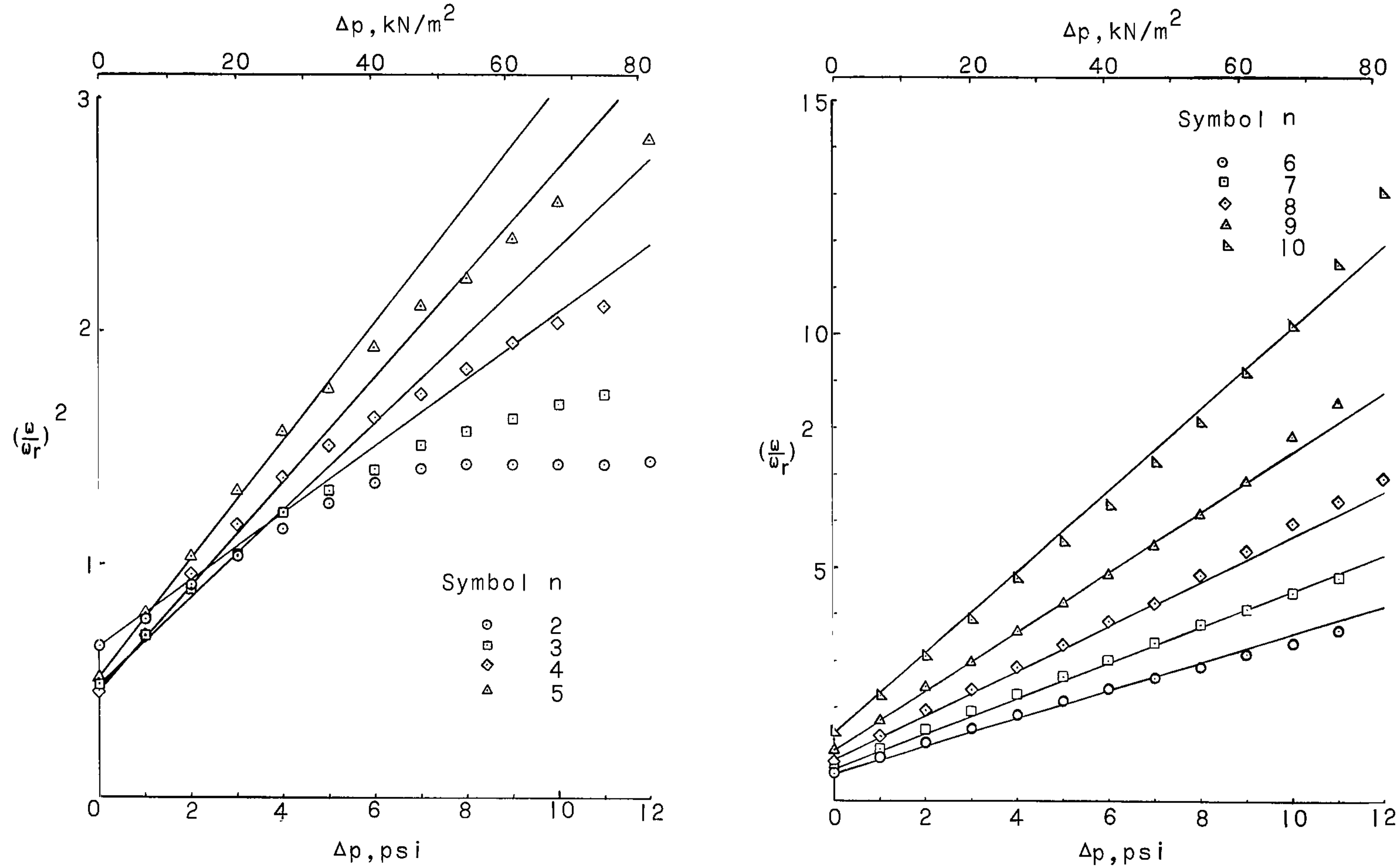

(a) n = 2 to 5.

(b) n = 6 to 10.

Figure 4.- Experimental variation of squared nondimensional frequency with differential pressure. ω_r = 731 Hz.

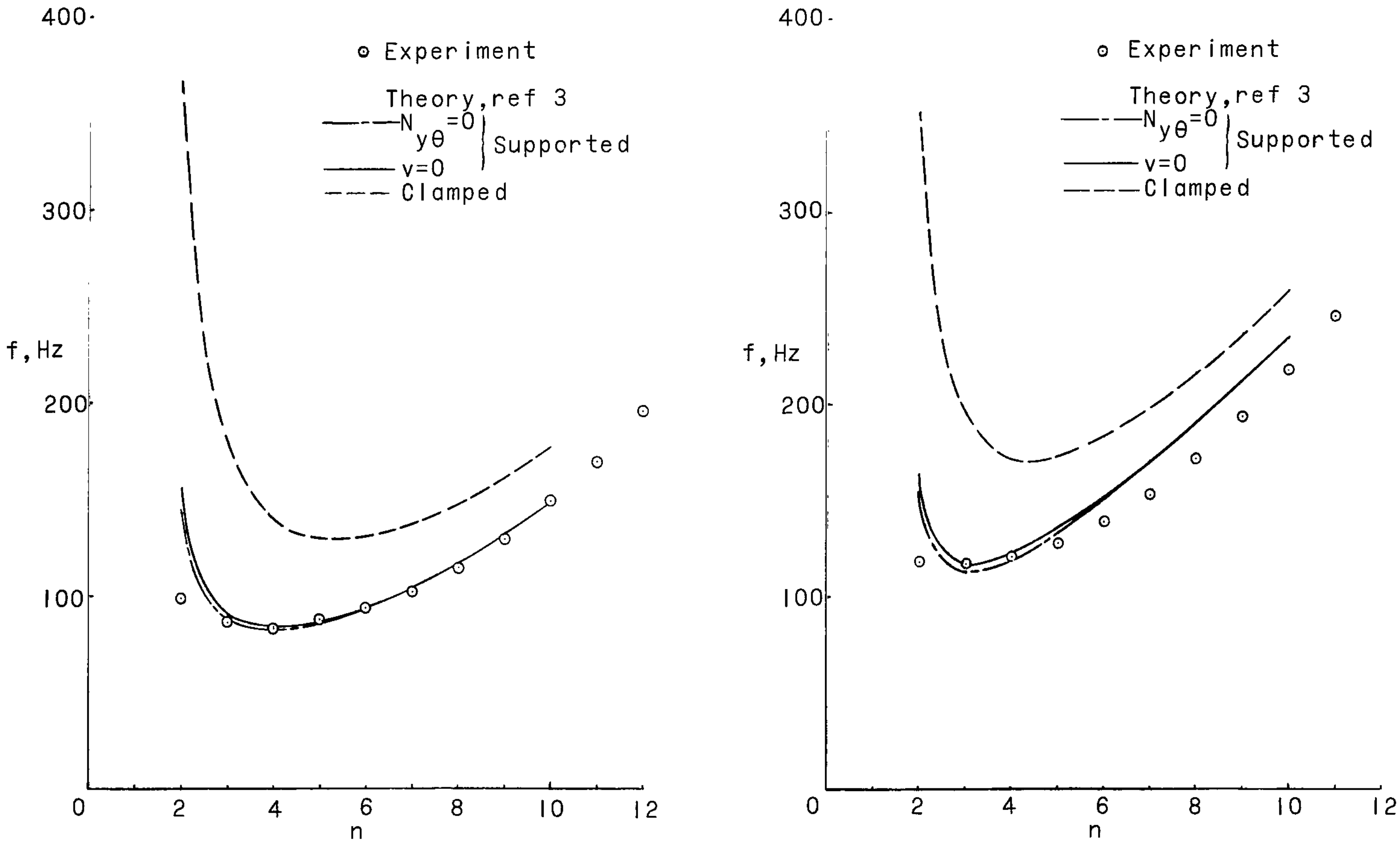

(a) $\Delta p = 0$.

(b) $\Delta p = 14\ kN/m^2$ (2 psi).

Figure 5.- Comparison of theoretical and experimental frequencies. m = 1.

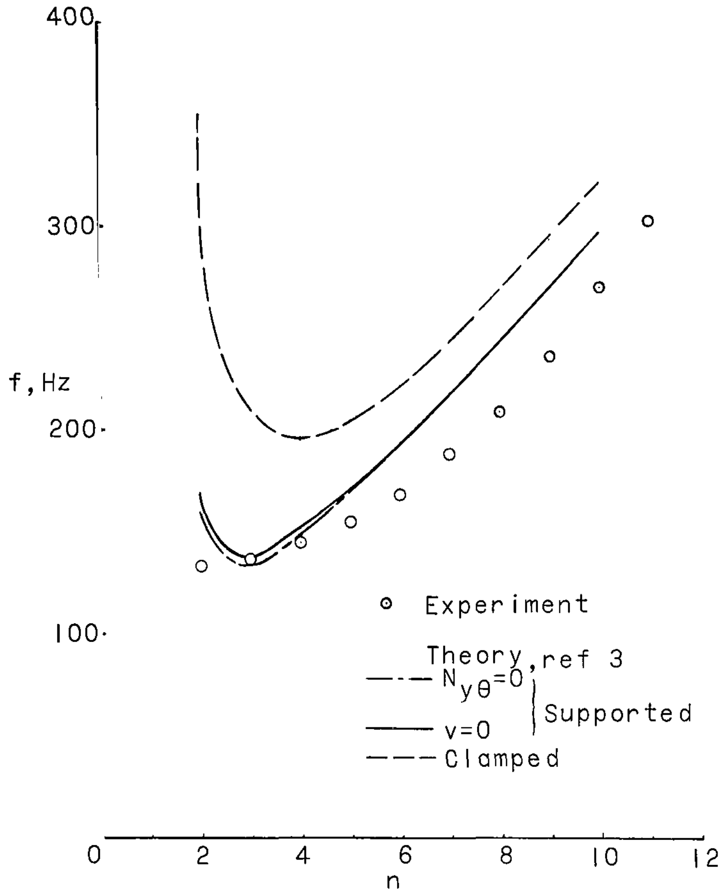

(c) Δp = 28 kN/m^2 (4 psi).

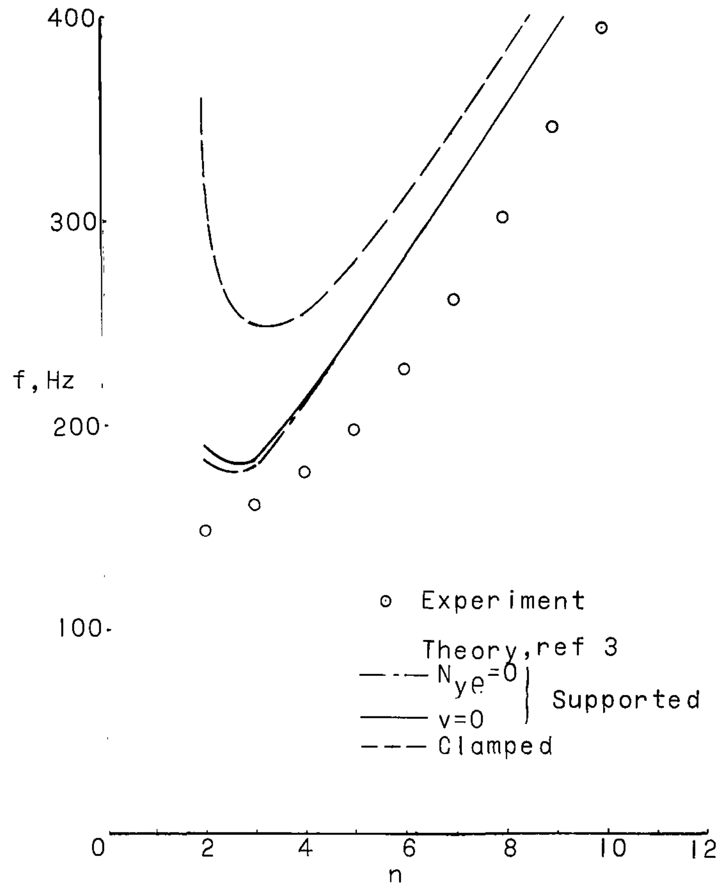

(d) Δp = 69 kN/m^2 (10 psi).

Figure 5.- Concluded.

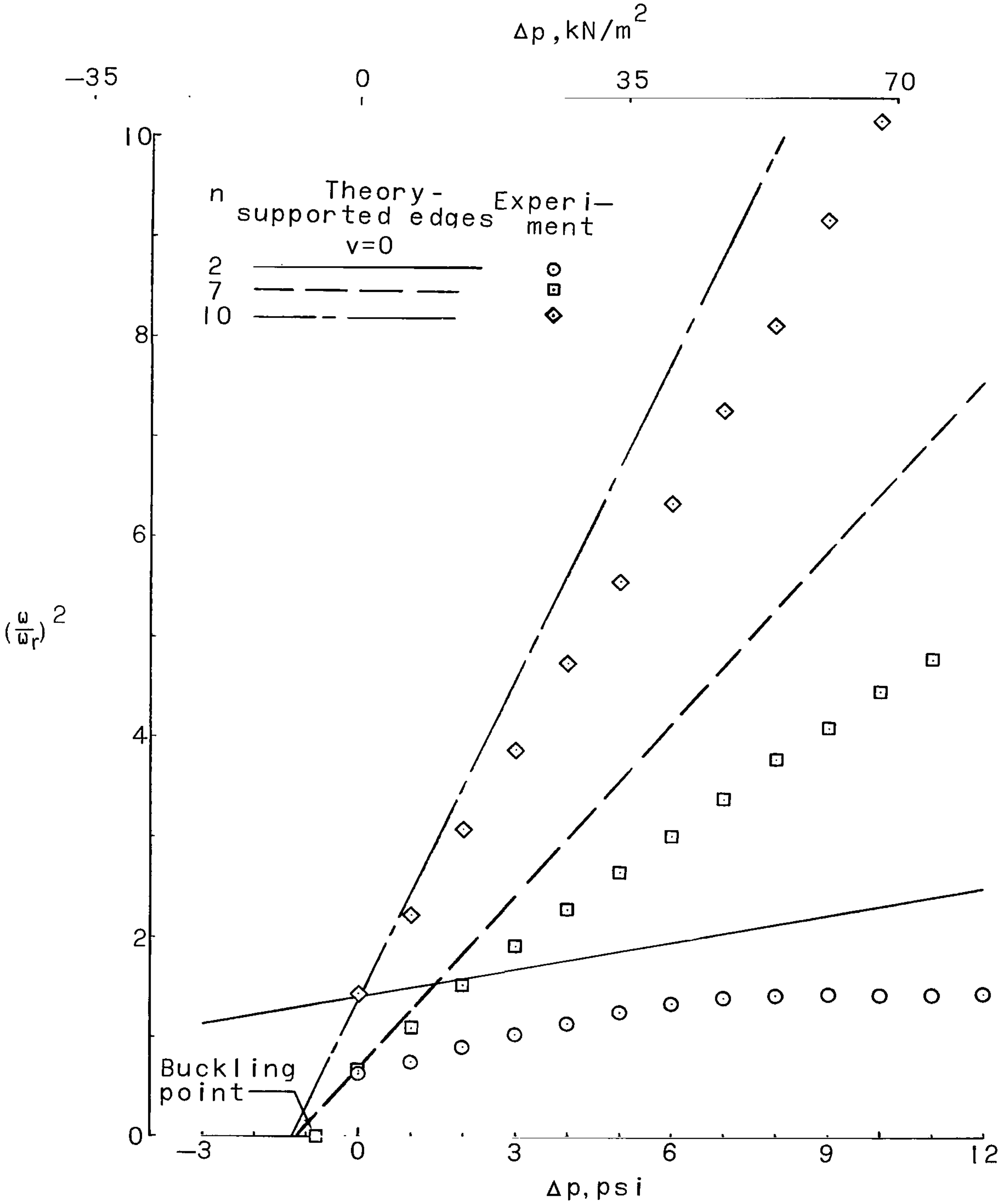

Figure 6.- Comparison of theoretical and experimental variation of nondimensional frequency squared with differential pressure. $m = 1$; $\omega_r = 731$ Hz.

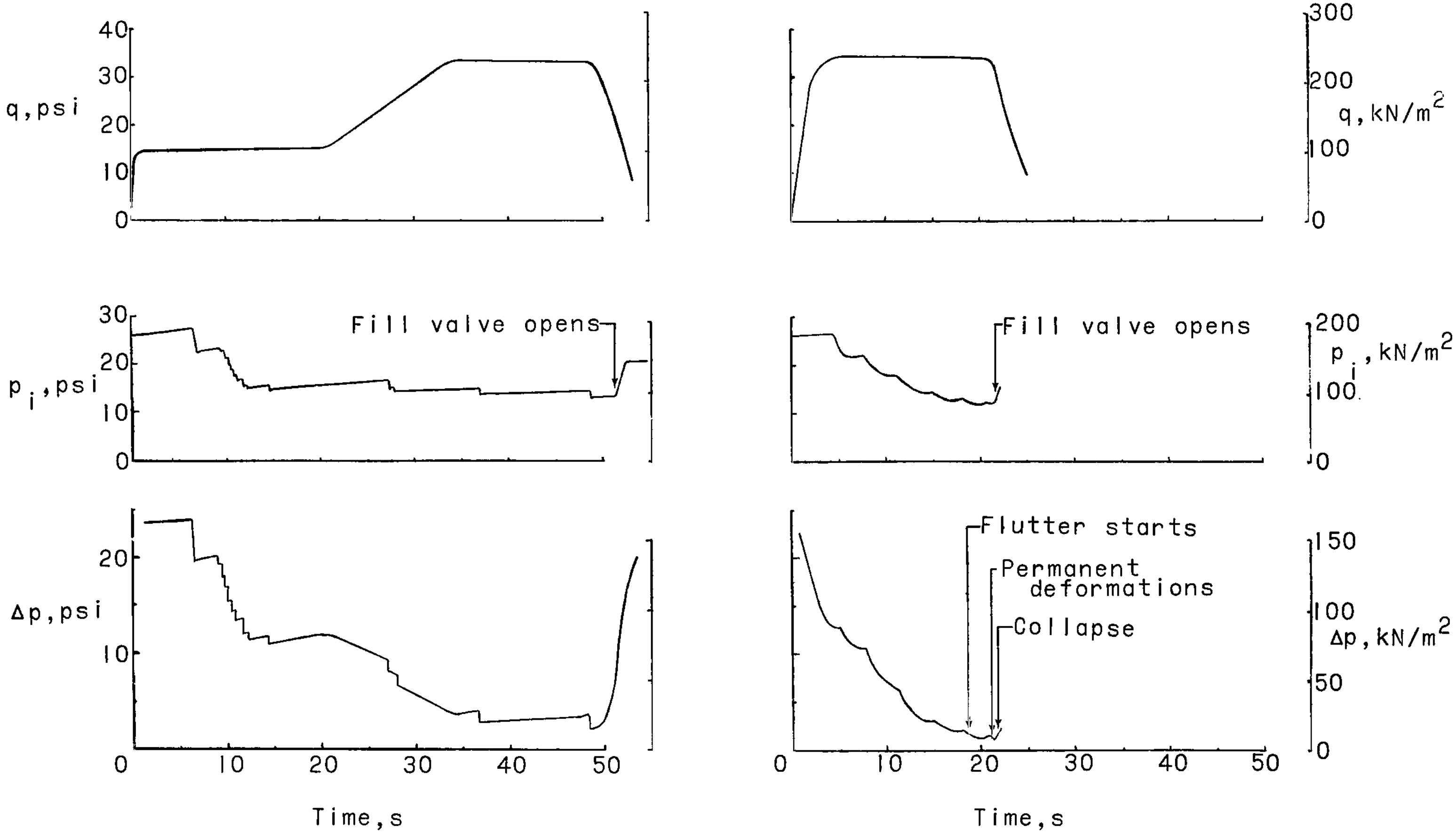

(a) Run 1. (b) Run 2.

Figure 7.- Free-stream dynamic pressure, internal pressure, and differential pressure time histories.

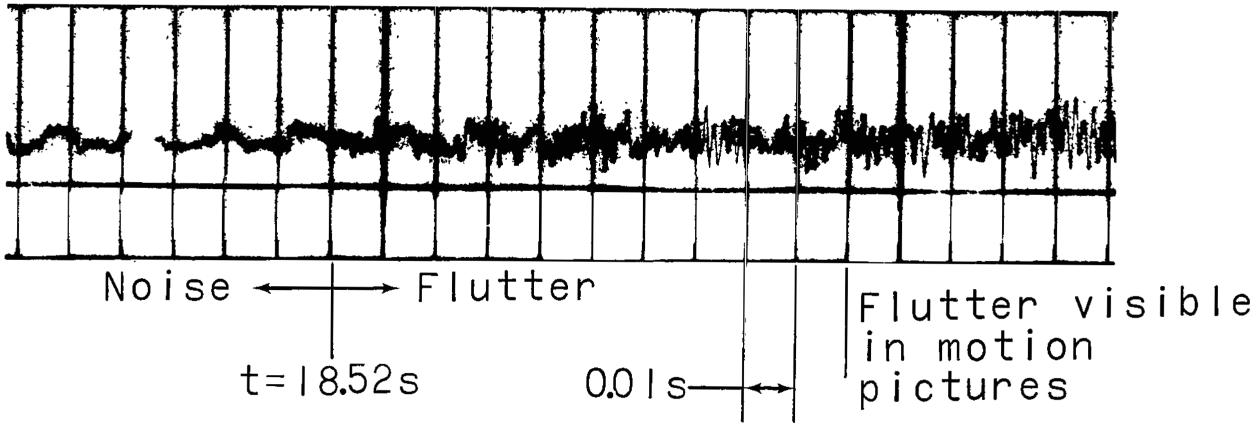

Figure 8.- Sample deflectometer record showing change from noise to flutter.

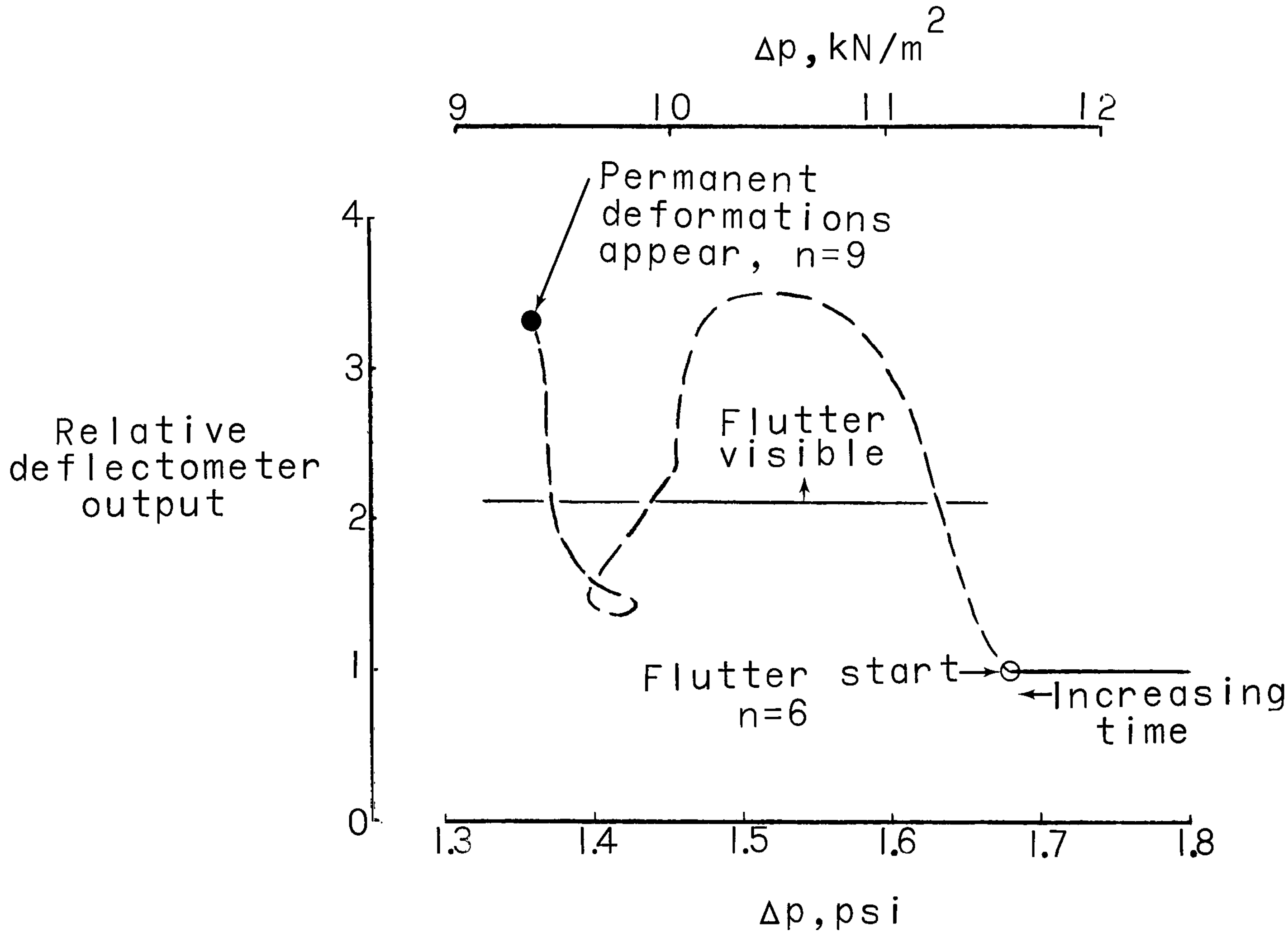

Figure 9.- Variation of relative deflectometer output and film data with internal pressure at end of run 2.

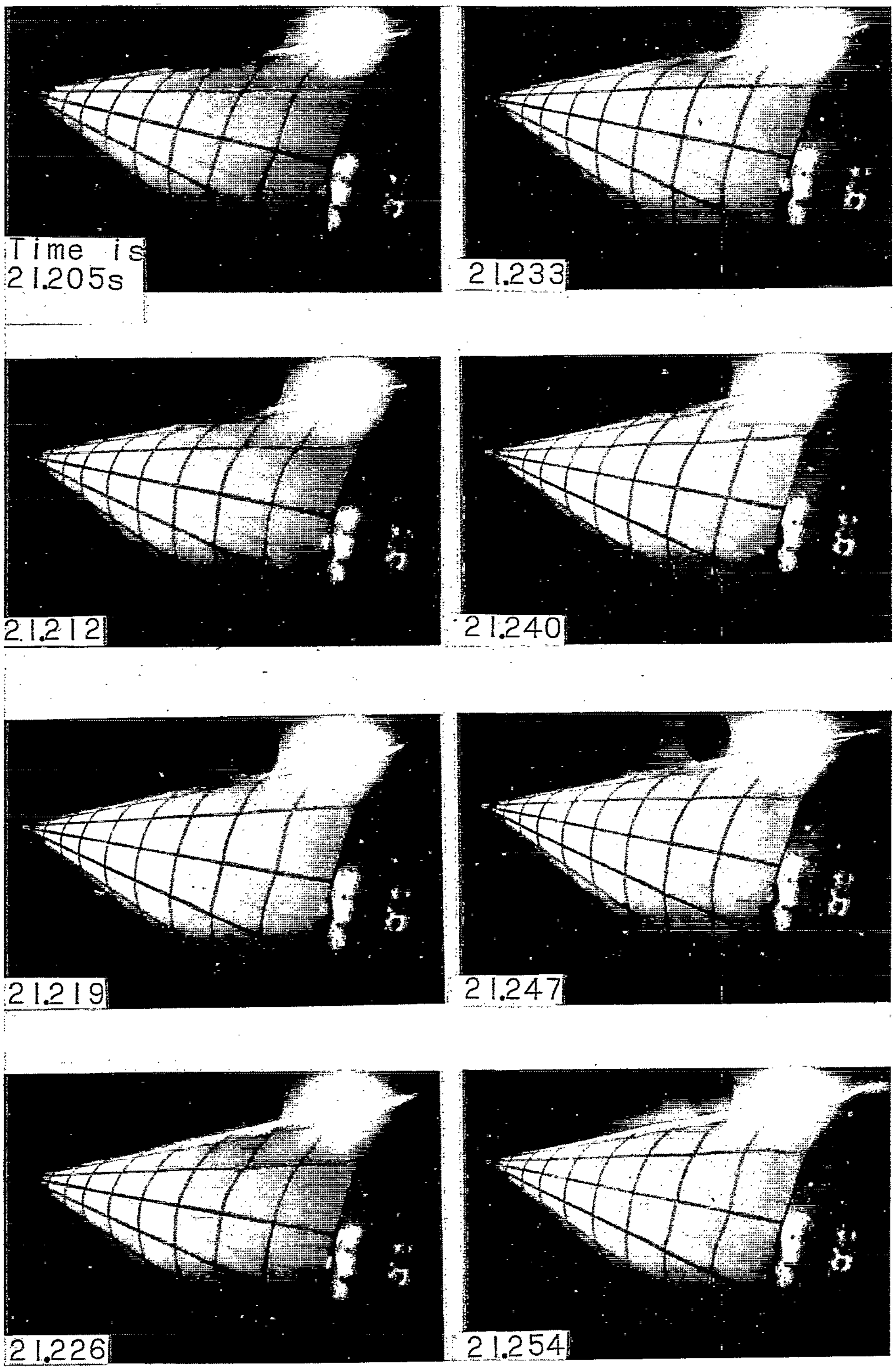

L-70-8033

Figure 10.- Motion-picture frames showing flutter and the occurrence of permanent deformations about 21.23 seconds into run 2.

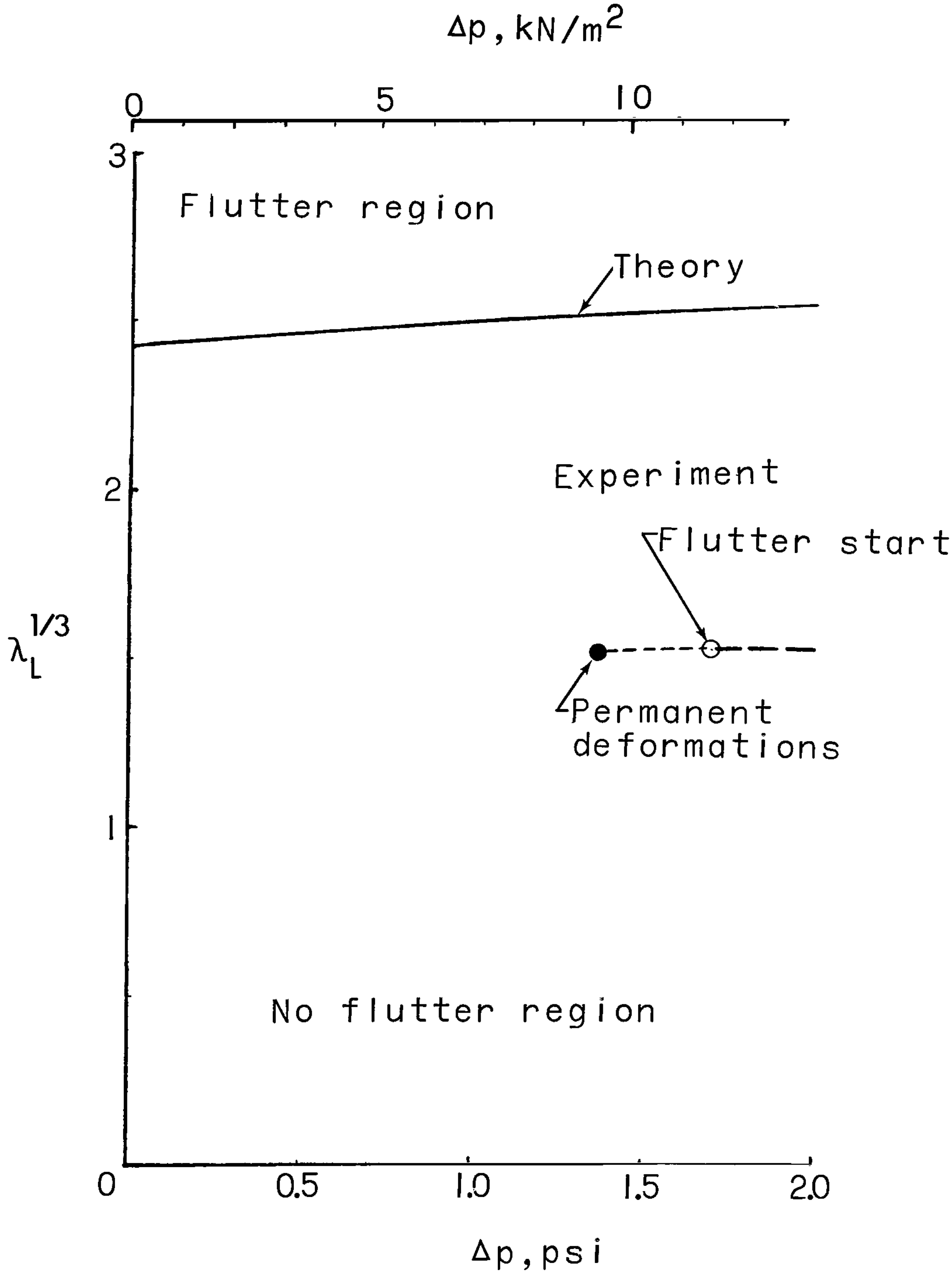

Figure 11.- Comparison of theoretical and experimental flutter results.

NASA-Langley, 1971 —— 32 L-7345